

Mixing asymmetries in B meson systems, the $D0$ like-sign dimuon asymmetry, and generic new physics

F. J. Botella,^{1,*} G. C. Branco,^{2,†} M. Nebot,^{2,‡} and A. Sánchez^{1,§}

¹*Departament de Física Teòrica and IFIC, Universitat de València-CSIC, E-46100 Burjassot, Spain*

²*Centro de Física Teórica de Partículas and Departamento de Física Instituto Superior Técnico, Universidade de Lisboa, Avenida Rovisco Pais, P-1049-001 Lisboa, Portugal*

(Received 28 October 2014; published 12 February 2015)

The measurement of a large like-sign dimuon asymmetry A_{SL}^b by the $D0$ experiment at the Tevatron departs noticeably from Standard Model (SM) expectations and it may be interpreted as a hint of physics beyond the Standard Model contributing to $\Delta B \neq 0$ transitions. In this work we analyze how the natural suppression of A_{SL}^b in the SM can be circumvented by new physics. We consider generic Standard Model extensions where the charged current mixing matrix is enlarged with respect to the usual 3×3 unitary Cabibbo-Kobayashi-Maskawa matrix, and show how, within this framework, a significant enhancement over Standard Model expectations for A_{SL}^b is easily reachable through enhancements of the semileptonic asymmetries A_{SL}^d and A_{SL}^s of both $B_d^0-\bar{B}_d^0$ and $B_s^0-\bar{B}_s^0$ systems. Despite being insufficient to reproduce the $D0$ measurement, such deviations from SM expectations may be probed by the LHCb experiment.

DOI: 10.1103/PhysRevD.91.035013

PACS numbers: 12.60.-i, 12.15.Ff, 11.30.Er, 14.65.Jk

I. INTRODUCTION

Flavor physics and CP violation provide a magnificent laboratory to probe our fundamental understanding of nature and to test, at unprecedented levels, the Standard Model (SM) and any of its extensions. The impact of the B factories $BABAR$ and $Belle$ operating at e^+e^- machines, of the $D0$ and CDF experiments operating at the Tevatron and lately of the $ATLAS$, CMS and $LHCb$ experiments at the LHC, is of paramount importance.

Among the plethora of results on CP -violating phenomena, the measurement by the $D0$ Collaboration [1] of the like-sign dimuon asymmetry A_{SL}^b has received much attention. Schematically, (i) $b\bar{b}$ pairs are strongly produced, (ii) they hadronize into B_d or B_s mesons/antimesons and (iii) they decay weakly. Semileptonic decays are flavor specific and “tag” the nature of the decaying B depending on the charge of the produced lepton ℓ : meson for ℓ^+ or antimeson for ℓ^- . If it were not for $B_q-\bar{B}_q$ oscillations, both decays could not produce leptons [2] of the same charge. In the presence of $B_q-\bar{B}_q$ oscillations, such like-sign muon double decay channels occur, and one defines the asymmetry [3]

$$A_{\text{SL}}^b = \frac{N^{++} - N^{--}}{N^{++} + N^{--}}, \quad (1)$$

with N^{++} (N^{--}) denoting the number of events with both B mesons decaying to μ^+ (μ^-). The values reported by the $D0$

Collaboration [1] are around “ 3σ ” away from Standard Model expectations, and this triggered intense activity to explore the potential of an ample variety of models beyond the SM to produce such values. As A_{SL}^b can be expressed in terms of the individual asymmetries A_{SL}^d and A_{SL}^s of $B_d^0-\bar{B}_d^0$ and $B_s^0-\bar{B}_s^0$ systems [4], it is customary to discuss in terms of them. In particular, since it is a common thought that the B factories have left little space for new physics (NP) to contribute new sources of CP violation in the $B_d^0-\bar{B}_d^0$ system, A_{SL}^s has attracted more attention in recent times [5]. New physics has been invoked to modify the dispersive mixing amplitudes $M_{12}^{(d,s)}$ and/or the absorptive ones $\Gamma_{12}^{(d,s)}$ in specific scenarios, such as supersymmetric extensions of the SM [6], extra dimensions [7], Z' models [8], left-right models [9], extended scalar sectors [10], axigluon exchange [11] or additional fermion generations [12]. New physics in A_{SL}^b has also been explored through model-independent analyses [13,14] or through NP modifying highly suppressed (within the SM) additional contributions [15]. This article is organized as follows. In Sec. II we review the well-known SM prediction for the semileptonic asymmetries A_{SL}^d and A_{SL}^s , and the dimuon asymmetry A_{SL}^b . In Sec. III we revisit a model-independent analysis where new physics is allowed to modify the mixing amplitudes $M_{12}^{(q)}$, and show how the previous asymmetries can be significantly larger than SM expectations. In Sec. IV we consider NP scenarios where the mixing matrix is not the usual 3×3 unitary Cabibbo-Kobayashi-Maskawa (CKM), but an enlarged one, and thus study for the first time how the values that the asymmetries of interest can span, differ from the SM ones. We also analyze the prospects to eventually distinguish if the mixing matrix is

*fbotella@uv.es

†gbranco@tecnico.ulisboa.pt

‡nebot@cftp.ist.utl.pt

§asanchez@ific.uv.es

3×3 unitary or not. In the last section we present our conclusions.

II. MIXING IN B_d AND B_s MESON SYSTEMS

Under general conditions, the time evolution of the B_q^0 - \bar{B}_q^0 systems $q = d, s$ is described by an effective weak Hamiltonian $\mathcal{H}_{(q)}$ according to the Schrödinger equation [16]

$$i \frac{d}{dt} \begin{pmatrix} B_q(t) \\ \bar{B}_q(t) \end{pmatrix} = \mathcal{H}_{(q)} \begin{pmatrix} B_q(t) \\ \bar{B}_q(t) \end{pmatrix}. \quad (2)$$

$\mathcal{H}_{(q)}$ has Hermitian and anti-Hermitian parts $M^{(q)}$ and $-i\Gamma^{(q)}/2$:

$$\mathcal{H}_{(q)} = M^{(q)} - \frac{i}{2}\Gamma^{(q)}, \quad M^{(q)} = M^{(q)\dagger}, \quad \Gamma^{(q)} = \Gamma^{(q)\dagger}. \quad (3)$$

In the Standard Model, the dispersive part $M_{12}^{(q)}$ of the transition amplitude $B_q \rightarrow \bar{B}_q$ is dominated by one loop box diagrams with virtual t quarks and W bosons [17]

$$[M_{12}^{(q)}]_{\text{SM}} = \frac{G_F^2 M_W^2}{12\pi^2} M_{B_q} f_{B_q}^2 B_{B_q} \eta_B (V_{tb} V_{tq}^*)^2 S_0(x_t). \quad (4)$$

On the other hand, the absorptive part $\Gamma_{12}^{(q)}$ is dominated by intermediate real (on-shell) u and c quarks. The corresponding SM short-distance prediction is more involved [18,19]: a heavy quark expansion is carried out, yielding $\Gamma_{12}^{(q)}$ as an expansion in $\alpha_s(m_b)$ and Λ/m_b . Focusing on the flavor structure, it has in general the following form

$$\frac{\Gamma_{12}^{(q)}}{M_{12}^{(q)}} = - \left[\frac{\Gamma_{12}^{cc}}{M_{12}^{(q)}} (V_{cb} V_{cq}^*)^2 + 2 \frac{\Gamma_{12}^{uc}}{M_{12}^{(q)}} (V_{ub} V_{uq}^* V_{cb} V_{cq}^*) + \frac{\Gamma_{12}^{uu}}{M_{12}^{(q)}} (V_{ub} V_{uq}^*)^2 \right], \quad (5)$$

and in particular in the SM the flavor structure is

$$\begin{aligned} \left[\frac{\Gamma_{12}^{(q)}}{M_{12}^{(q)}} \right]_{\text{SM}} &\propto \Gamma_{12}^{cc} \frac{(V_{cb} V_{cq}^*)^2}{(V_{tb} V_{tq}^*)^2} + 2\Gamma_{12}^{uc} \frac{V_{ub} V_{uq}^* V_{cb} V_{cq}^*}{(V_{tb} V_{tq}^*)^2} \\ &+ \Gamma_{12}^{uu} \frac{(V_{ub} V_{uq}^*)^2}{(V_{tb} V_{tq}^*)^2}. \end{aligned} \quad (6)$$

It is important to notice that, in terms of the weak interactions, the coefficients Γ_{12}^{uu} , Γ_{12}^{uc} and Γ_{12}^{cc} are dominated by tree level contributions. We can then rely on Eq. (5) without qualms about new physics contributions invalidating it: only if a given scenario beyond the Standard Model

can give competing contributions to tree level SM predictions, should we worry and consider a specific analysis. The coefficients Γ_{12}^{ab} are in turn

$$-\Gamma_{12}^{cc} = c, \quad -2\Gamma_{12}^{uc} = 2c - a, \quad -\Gamma_{12}^{uu} = b + c - a, \quad (7)$$

where [19]

$$\begin{aligned} a &= (10.5 \pm 1.8) \times 10^{-4}, \\ b &= (0.2 \pm 0.1) \times 10^{-4}, \\ c &= (-53.3 \pm 12.0) \times 10^{-4}. \end{aligned} \quad (8)$$

It is important to stress that in an expansion in powers of $(m_c/m_b)^2$, only c is present at zeroth order. Then, unitarity of the CKM mixing matrix, implying the orthogonality condition $V_{ub} V_{uq}^* + V_{cb} V_{cq}^* + V_{tb} V_{tq}^* = 0$, can be used to write

$$\left[\frac{\Gamma_{12}^{(q)}}{M_{12}^{(q)}} \right]_{\text{SM}} = K_{(q)} \left[c + a \frac{V_{ub} V_{uq}^*}{V_{tb} V_{tq}^*} + b \left(\frac{V_{ub} V_{uq}^*}{V_{tb} V_{tq}^*} \right)^2 \right], \quad (9)$$

where

$$K_{(q)} = \frac{12\pi^2}{M_{B_q} f_{B_q}^2 B_{B_q} G_F^2 M_W^2 \eta_B S_0(x_t)}.$$

$\Gamma_{12}^{(q)}/M_{12}^{(q)}$ is accessed through two observables; at leading order in $\Gamma_{12}^{(q)}/M_{12}^{(q)}$ powers, one has

$$-\frac{\Delta\Gamma_q}{\Delta M_{B_q}} = \text{Re} \left(\frac{\Gamma_{12}^{(q)}}{M_{12}^{(q)}} \right), \quad A_{\text{SL}}^q = \text{Im} \left(\frac{\Gamma_{12}^{(q)}}{M_{12}^{(q)}} \right). \quad (10)$$

The real part $\text{Re}(\Gamma_{12}^{(q)}/M_{12}^{(q)})$ controls the width difference between the eigenstates of $\mathcal{H}_{(q)}$. The imaginary part $\text{Im}(\Gamma_{12}^{(q)}/M_{12}^{(q)})$ is genuinely CP violating and only involves mixing amplitudes; as anticipated, it is accessed through asymmetries in flavor-specific, semileptonic decays. The SM expectations for those observables, with the inputs in Table I (Appendix A), are

$$\begin{aligned} [A_{\text{SL}}^d]_{\text{SM}} &= (-4.2 \pm 0.7) \times 10^{-4}, \\ [\Delta\Gamma_d]_{\text{SM}} &= (2.60 \pm 0.25) \times 10^{-3} \text{ ps}^{-1}, \\ [A_{\text{SL}}^s]_{\text{SM}} &= (2.0 \pm 0.3) \times 10^{-5}, \\ [\Delta\Gamma_s]_{\text{SM}} &= (0.090 \pm 0.008) \text{ ps}^{-1}. \end{aligned} \quad (11)$$

The following comments are in order:

- (i) both A_{SL}^d and A_{SL}^s are small, $\mathcal{O}(10^{-4})$ and $\mathcal{O}(10^{-5})$ respectively, with room for variation at the $\pm 20\%$ level. This smallness can be traced back to the

$(m_c/m_b)^2$ suppression in Eq. (9): the leading contribution proportional to c is real and does not contribute to the semileptonic asymmetries; furthermore, since the hierarchy of the CKM matrix gives

$$\left| \frac{V_{ud}^* V_{ub}}{V_{td}^* V_{tb}} \right| \simeq 0.40, \quad \arg \left(\frac{V_{ud}^* V_{ub}}{V_{td}^* V_{tb}} \right) \simeq -1.57, \quad (12)$$

$$\left| \frac{V_{us}^* V_{ub}}{V_{ts}^* V_{tb}} \right| \simeq 0.02, \quad \arg \left(\frac{V_{us}^* V_{ub}}{V_{ts}^* V_{tb}} \right) \simeq \pi - 1.18, \quad (13)$$

one could expect $|A_{\text{SL}}^d| \gg |A_{\text{SL}}^s|$.

- (ii) $\Delta\Gamma_d$ is $\mathcal{O}(10^{-3}) \text{ ps}^{-1}$ and $\Delta\Gamma_s$ is $\mathcal{O}(10^{-1}) \text{ ps}^{-1}$: while $\Gamma_d \simeq \Gamma_s \simeq (1.5 \text{ ps})^{-1}$, the hierarchy in $\Delta\Gamma_d$ and $\Delta\Gamma_s$ can be anticipated with the leading term in Eq. (9), giving $\Delta\Gamma_s/\Delta M_{B_s} \sim \Delta\Gamma_d/\Delta M_{B_d}$.

Underlying this simple SM analysis are two important assumptions:

- (1) $M_{12}^{(q)}$ is dominated by a single weak amplitude (the one with virtual top quarks);
- (2) the CKM matrix is 3×3 unitary.

Another interesting possibility is to rewrite the flavor structure of Eq. (5), as done in [20], in terms of *a priori* measurable quantities, as we now illustrate for $q = d$. Since the mass difference [21] between the eigenstates of $\mathcal{H}_{(d)}$ is $\Delta M_{B_d} = 2|M_{12}^{(d)}|$, and the ‘‘golden’’ time-dependent CP asymmetry $A_{J/\Psi K_S}$ in $B_d \rightarrow J/\Psi K_S$ is controlled by $\arg(M_{12}^{(d)})$, one can use

$$M_{12}^{(d)} = \frac{\Delta M_{B_d}}{2} e^{i2\bar{\beta}}, \quad (14)$$

with the effective phase $\bar{\beta}$ given by $A_{J/\Psi K_S} \equiv \sin(2\bar{\beta})$, to rewrite

$$\begin{aligned} \frac{\Gamma_{12}^{(d)}}{M_{12}^{(d)}} &= \frac{2}{\Delta M_{B_d}} [c e^{-i2\bar{\beta}} (|V_{cb} V_{cd}^*| - |V_{ub} V_{ud}^*| e^{-i\gamma})^2 \\ &\quad + a |V_{ub} V_{ud}^*| e^{-i(2\bar{\beta}+\gamma)} (|V_{cb} V_{cd}^*| - |V_{ub} V_{ud}^*| e^{-i\gamma}) \\ &\quad + b |V_{ub} V_{ud}^*|^2 e^{-i2(\bar{\beta}+\gamma)}]. \end{aligned} \quad (15)$$

We use the physical rephasing invariant phases [16] $\gamma \equiv \arg(-V_{ud} V_{ub}^* V_{cb} V_{cd}^*)$ and $\beta \equiv \arg(-V_{cd} V_{cb}^* V_{tb} V_{td}^*)$, even though in the SM $\bar{\beta} = \beta$, we introduce $\bar{\beta}$ for later use since it is directly related to an observable. Equation (15) provides a particularly interesting expression [22] for $\Gamma_{12}^{(d)}/M_{12}^{(d)}$. It involves (i) tree level CKM moduli $|V_{ub}|$, $|V_{ud}|$, $|V_{cb}|$ and $|V_{cd}|$, (ii) the mass difference ΔM_{B_d} , and (iii) the phases $2\bar{\beta}$, $2\bar{\beta} + \gamma$ and $2(\bar{\beta} + \gamma)$. All of them are, in principle, directly measurable [23] and furthermore, if new

physics contributes to $\Delta B = 2$ transitions, it can manifest through nonstandard values of the mass difference ΔM_{B_d} or the mixing phase $2\bar{\beta}$, which are automatically incorporated into Eq. (15); the remaining quantities are, in terms of weak interactions, *tree level*, hence *a priori* safe from potential contributions from new physics. Analogous expressions for the $B_s^0\text{-}\bar{B}_s^0$ case can be readily obtained:

$$\begin{aligned} \frac{\Gamma_{12}^{(s)}}{M_{12}^{(s)}} &= \frac{2}{\Delta M_{B_s}} [c e^{i2\bar{\beta}_s} (|V_{cb} V_{cs}^*| + |V_{ub} V_{us}^*| e^{-i\gamma})^2 \\ &\quad - a |V_{ub} V_{us}^*| e^{i(2\bar{\beta}_s-\gamma)} (|V_{cb} V_{cs}^*| + |V_{ub} V_{us}^*| e^{-i\gamma}) \\ &\quad + b |V_{ub} V_{us}^*|^2 e^{i2(\bar{\beta}_s-\gamma)}]. \end{aligned} \quad (16)$$

For the $B_s^0\text{-}\bar{B}_s^0$ system, the ‘‘golden’’ decay channel is $B_s \rightarrow J/\Psi \Phi$ and the corresponding time-dependent CP asymmetry is $A_{J/\Psi \Phi} \equiv \sin \bar{\beta}_s$.

The $(m_c/m_b)^2$ suppression of A_{SL}^d and A_{SL}^s within the SM manifests itself in Eq. (15) and in Eq. (16) through the unitarity relations

$$\begin{aligned} |V_{cb} V_{cd}^*| - |V_{ub} V_{ud}^*| e^{-i\gamma} &= |V_{tb} V_{td}^*| e^{-i\beta} \quad \text{and} \\ |V_{cb} V_{cs}^*| + |V_{ub} V_{us}^*| e^{-i\gamma} &= -|V_{tb} V_{ts}^*| e^{-i\beta_s}. \end{aligned} \quad (17)$$

Following the previous discussion of the semileptonic asymmetries A_{SL}^d and A_{SL}^s , it is easy to grasp how dramatically the dimuon asymmetry observed by D0 [1] *cannot* be obtained within the SM. The dimuon asymmetry A_{SL}^b is essentially a weighted combination of A_{SL}^d and A_{SL}^s ,

$$A_{\text{SL}}^b = \frac{A_{\text{SL}}^d + g A_{\text{SL}}^s}{1 + g} \quad (18)$$

where

$$g = f \frac{\Gamma_d (1 - y_s^2)^{-1} - (1 + x_s^2)^{-1}}{\Gamma_s (1 - y_d^2)^{-1} - (1 + x_d^2)^{-1}}, \quad y_q = \frac{\Delta\Gamma_q}{2\Gamma_q}, \quad x_q = \frac{\Delta M_{B_q}}{\Gamma_q}. \quad (19)$$

The $B_s\text{-}B_d$ fragmentation fraction ratio in the B sample is $f = 0.269 \pm 0.015$. Numerically $g \sim 1$ and thus A_{SL}^d and A_{SL}^s have similar weights in Eq. (18).

With $A_{\text{SL}}^s \sim 2 \times 10^{-5}$, A_{SL}^b is dominated by $A_{\text{SL}}^d \sim -5 \times 10^{-4}$ and the SM expectation turns out to be

$$A_{\text{SL}}^b = (-2.40 \pm 0.45) \times 10^{-4}. \quad (20)$$

The values quoted by the D0 Collaboration are $A_{\text{SL}}^b = (-7.87 \pm 1.72 \pm 0.93) \times 10^{-3}$ and $A_{\text{SL}}^b = (-4.96 \pm 1.53 \pm 0.72) \times 10^{-3}$ in [1], so the disagreement with SM expectations, as anticipated, is around the 3σ level. It is important to stress again that the almost $\mathcal{O}(10^{-2})$ scale of that measured value is 20 times larger than SM expectations.

On the other hand, the LHCb Collaboration has recently started to measure the semileptonic asymmetry A_{SL}^s [4]; additional results concerning $A_{\text{SL}}^s \pm A_{\text{SL}}^d$ are also expected [24]. If the D0 measurement is to be interpreted as a clear signal of new physics, LHCb results, in particular $A_{\text{SL}}^s \pm A_{\text{SL}}^d$, should necessarily depart from the SM expectations

$$\begin{aligned} A_{\text{SL}}^s + A_{\text{SL}}^d &= (-4.0 \pm 0.7) \times 10^{-4}, \\ A_{\text{SL}}^s - A_{\text{SL}}^d &= (4.1 \pm 0.7) \times 10^{-4}. \end{aligned} \quad (21)$$

In this section we have analyzed the details of the SM expectations for observables genuinely related to mixing in neutral B_d and B_s systems, including the ‘‘problematic’’ asymmetry measured at the Tevatron. Those are, in any case, well-known results, but analyzing them in detail, in particular how the use of 3×3 unitarity and the dominance of the top quark contribution in $M_{12}^{(q)}$ are central in the SM suppressed expectation, paves the way to understand the changes to the picture which one encounters when moving beyond the SM.

III. NEW PHYSICS WITHIN 3×3 UNITARITY

In order to move beyond the SM, a general model-independent analysis of NP in the flavor sector could start by considering the effective Hamiltonians describing a set of relevant weak transitions. Model independence would be achieved by allowing all independent Wilson coefficients to depart from SM values. This task would not only be daunting, but would also be very difficult to extract meaningful information from it, since the NP parameters controlling the generalized Wilson coefficients would typically show a high degree of degeneracy (not to mention the experimental accuracy required to single out any interesting feature in such a scenario). One can consider simpler, yet interesting alternatives, by focusing on a few relevant operators that enter multiple observables. In addition, since the SM flavor picture is essentially correct, it is legitimate to circumscribe NP deviations to the Wilson coefficients of operators that do not arise at tree level in the SM. An approach that has been rather popular in recent times [20,25] focuses on meson mixings. Since the dispersive amplitudes $M_{12}^{(q)}$ arise at the loop level in the SM, they are appropriate candidates to be polluted by new physics; the effect of having new contributions may be parametrized in the following manner (with r_q , ϕ_q , new, independent parameters):

$$M_{12}^{(q)} = [M_{12}^{(q)}]_{\text{SM}} r_q^2 e^{-i2\phi_q}. \quad (22)$$

Deviations from $(r_q, \phi_q) = (1, 0)$ describe new physics in the mixing of B_q mesons. Equation (22) has several advantages. Since $2|M_{12}^{(q)}| = \Delta M_{B_q}$, one concludes that

- (i) the prediction for ΔM_{B_q} is directly modified, with respect to the SM, by r_q , but unaffected by ϕ_q ,
- (ii) ϕ_q directly modifies, in a common way, the SM prediction for observables where the phase of the (dispersive) mixing enters: this is the case, for example, of the ‘‘golden’’ time-dependent CP asymmetries in $B_d^0 \rightarrow J/\Psi K_S$ and $B_s^0 \rightarrow J/\Psi \Phi$; these are insensitive to r_d and r_s .

This ‘‘factorization’’ of the effects of new physics is quite convenient [26].

In the SM, $M_{12}^{(q)}$ is controlled by a single dimension-six $\Delta B = 2$ effective operator; in Eq. (22), $r_q^2 e^{-i2\phi_q}$ can be interpreted as the factor modifying the corresponding Wilson coefficient in the presence of NP. However, notice that for specific models where r_d , r_s , ϕ_d and ϕ_s are not independent, the situation may be more involved.

The very first question one should address when considering Eq. (22) is whether this kind of modification could bring something *really* new to the SM picture presented in Sec. II. Naively, one would expect an affirmative answer. Nevertheless, since (i) $\Gamma_{12}^{(d)}$ and $\Gamma_{12}^{(s)}$ are tree level dominated and (ii) $M_{12}^{(d)}$ and $M_{12}^{(s)}$ are constrained by experimental information [27], modifying the picture may not be so straightforward. First of all, through Eq. (22), the predictions for the most important observables are modified according to

$$\Delta M_{B_d} = r_d^2 |V_{tb} V_{td}^*|^2 \frac{G_F^2 M_W^2}{6\pi^2} M_{B_d} f_{B_d}^2 B_{B_d} \eta_B S_0(x_t), \quad (23)$$

$$A_{J/\Psi K_S} = \sin(2\bar{\beta}) = \sin(2(\beta - \phi_d)), \quad (24)$$

$$\Delta M_{B_s} = r_s^2 |V_{tb} V_{td}^*|^2 \frac{G_F^2 M_W^2}{6\pi^2} M_{B_s} f_{B_s}^2 B_{B_s} \eta_B S_0(x_t), \quad (25)$$

$$A_{J/\Psi \Phi} = \sin(2\bar{\beta}_s) = \sin(2(\beta_s + \phi_s)), \quad (26)$$

where we have introduced for convenience the effective phases $\bar{\beta} \equiv \beta - \phi_d$ and $\bar{\beta}_s \equiv \beta_s + \phi_s$. Considering Eqs. (23)–(26), our skepticism takes a precise form: if the functional form of $\Gamma_{12}^{(q)}$ does not change, while $M_{12}^{(q)}$ obeys the same experimental constraints, how could $\Gamma_{12}^{(q)}/M_{12}^{(q)}$ differ from SM expectations?

Figure 1 displays the individual $\Delta\chi^2$ profiles of A_{SL}^d and A_{SL}^s corresponding to this NP scenario together with the SM ones (obtained using the same experimental constraints, the ones in Table I): there is little doubt that the simple modification in Eq. (22) allows for ample deviations from SM expectations. Consider for example the $B_d^0 - \bar{B}_d^0$ system.

With the following values,

$$2\phi_d \approx 0.20, \quad \beta \approx 0.47, \quad \gamma \approx 1.22, \quad 2(\beta + \gamma) \approx 3.36, \quad (27)$$

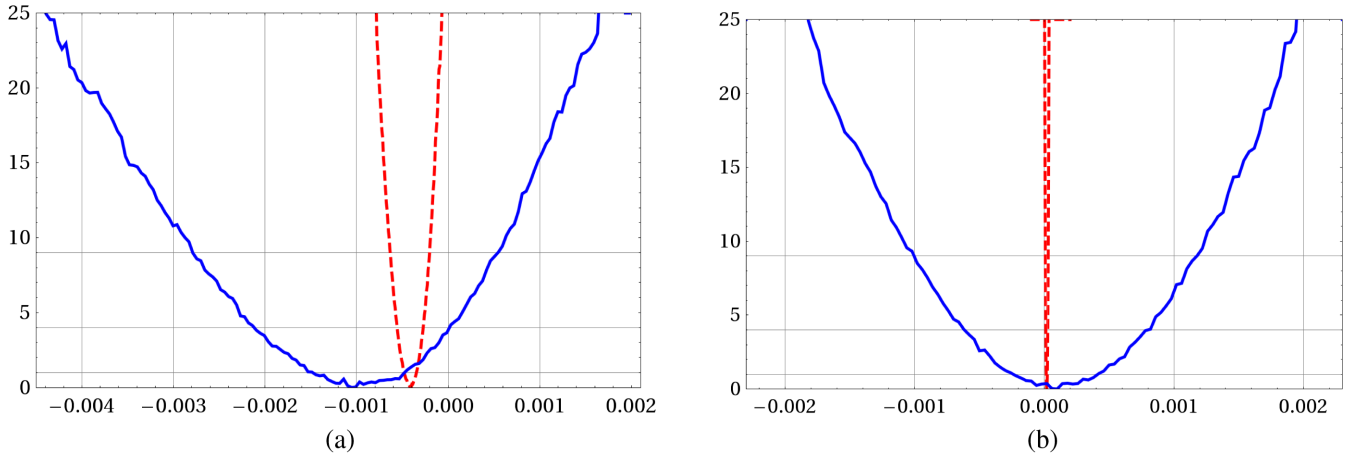


FIG. 1 (color online). $\Delta\chi^2$ profile of the semileptonic asymmetries A_{SL}^d and A_{SL}^s ; the blue line corresponds to the NP scenario—Eq. (22)—the red dashed line corresponds to the SM case. Notice that for A_{SL}^s the SM range is too narrow to be resolved on this scale. (a) $\Delta\chi^2$ vs A_{SL}^d . (b) $\Delta\chi^2$ vs A_{SL}^s .

$$|V_{ud}^* V_{ub}| \approx 4.22 \times 10^{-3}, \quad |V_{cd}^* V_{cb}| \approx 9.22 \times 10^{-3}, \quad (28)$$

one obtains

$$\Delta\Gamma_d = 3.25 \times 10^{-3} \text{ ps}^{-1} \quad \text{and} \quad A_{\text{SL}}^d = -1.92 \times 10^{-3}. \quad (29)$$

While $\Delta\Gamma_d$ is rather unchanged, the departure of A_{SL}^d from the value in Eq. (11) is quite significant: it is larger by a factor of 5. How can such a large enhancement be achieved? The main differences between the values in Eqs. (28) and (27) and the ones in the SM case, $\beta \approx 0.38$, $\gamma \approx 1.18$, $|V_{ud}^* V_{ub}| \approx 3.46 \times 10^{-3}$ and $|V_{cd}^* V_{cb}| \approx 9.23 \times 10^{-3}$, are in $|V_{ub}|$ and β . In the SM, 3×3 unitarity of the CKM matrix, nicely illustrated by the usual bd unitarity triangle, forces $|V_{ub}|$ to be tightly related to β . This is indeed the cornerstone of the so-called *tensions* in the bd sector [28]. In this extended scenario, the situation is changed. While $|V_{ub}|$ is still directly obtained, and it may call for values larger than in the SM fit, the measurement of $A_{J/\psi K_S}$ fixes $\tilde{\beta}$ instead of β . The new parameter ϕ_d breaks the SM tight relation between $A_{J/\psi K_S}$ and $|V_{ub}|$ imposed by 3×3 unitarity and the dominance of the top quark contribution in $M_{12}^{(d)}$. This is sufficient to remove the $(m_c/m_b)^2$ suppression present in the imaginary part of $\Gamma_{12}^{(d)}/M_{12}^{(d)}$. We can read in Fig. 1(a) how far from SM expectations A_{SL}^d could be pushed: at 95% C.L. (that is, up to $\Delta\chi^2 = 4$), $A_{\text{SL}}^d \in [-3.3; -0.8] \times 10^{-3}$, to be compared with the SM 95% C.L. range $[-0.58; -0.29] \times 10^{-3}$. It is important to stress that although the presence of NP induces a departure in the phase of $M_{12}^{(d)}$ and in $|V_{ub}|$ with respect to

SM values at the 20%–30% level, A_{SL}^d is enhanced by a factor 4–5: it is *a priori* highly sensitive to the presence of NP in $M_{12}^{(d)}$ precisely because of the natural suppression present in the SM. The increase in $|V_{ub}|$ allowed by $\phi_d \neq 0$ may also enhance A_{SL}^s marginally—through the second, a -dependent term in Eq. (9)—however, the main source of potential deviation from SM expectations is simply $\phi_s \neq 0$: as illustrated in Fig. 1(b), A_{SL}^s can be lifted from values $\mathcal{O}(10^{-5})$ to values $\mathcal{O}(10^{-3})$.

One can indeed express [25] the asymmetry A_{SL}^q in this scenario as

$$\frac{\Gamma_{12}^{(q)}}{M_{12}^{(q)}} = \frac{e^{i2\phi_q}}{r_q^2} \left[\frac{\Gamma_{12}^{(q)}}{M_{12}^{(q)}} \right]_{\text{SM}} \Rightarrow A_{\text{SL}}^q = \frac{\cos(2\phi_q)}{r_q^2} [A_{\text{SL}}^q]_{\text{SM}} - \frac{\sin(2\phi_q)}{r_q^2} \left[\frac{\Delta\Gamma_q}{\Delta M_q} \right]_{\text{SM}}, \quad (30)$$

from which we can expect enhancements up to the 10^{-3} level in both $B_d^0\text{-}\bar{B}_d^0$ and $B_s^0\text{-}\bar{B}_s^0$ systems for phases $\phi_q \sim 0.1$. It is also interesting to represent the two-dimensional $\Delta\chi^2$ profiles of A_{SL}^q vs ϕ_q : in Figs. 2(a) and 2(b) we plot [29] A_{SL}^d vs $2\phi_d$ and A_{SL}^s vs $2\phi_s$, respectively.

Figure 2(a) shows how the A_{SL}^d departure from SM expectations relies on $2\phi_d \neq 0$. How $2\phi_s \neq 0$ can produce $\mathcal{O}(10^{-3})$ values for A_{SL}^s is clearly reflected in Fig. 2(b).

The previous analysis provides a clear picture of the deviations from SM expectations for the individual asymmetries A_{SL}^d and A_{SL}^s . Turning to the D0 asymmetry A_{SL}^0 , Fig. 3 shows the corresponding $\Delta\chi^2$ profile. Within 3σ it may reach values of -2.5×10^{-3} ; this means an enhancement of almost an order of magnitude with respect to the SM expectation in Eq. (18). However,

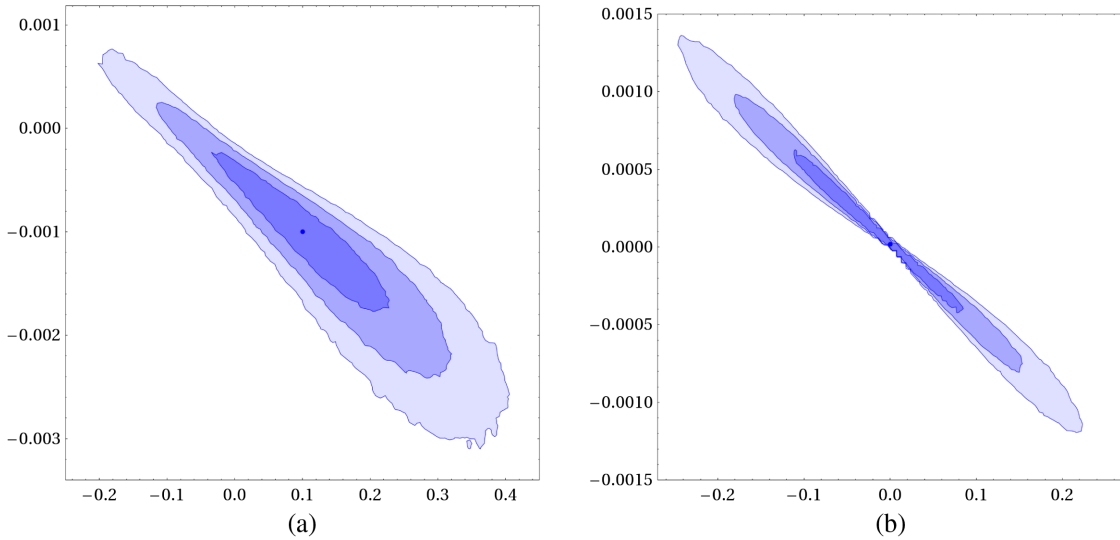


FIG. 2 (color online). $\Delta\chi^2$ profiles of A_{SL}^q vs $2\phi_q$; 68%, 95% and 99% C.L. regions are shown. (a) A_{SL}^d vs $2\phi_d$. (b) A_{SL}^s vs $2\phi_s$.

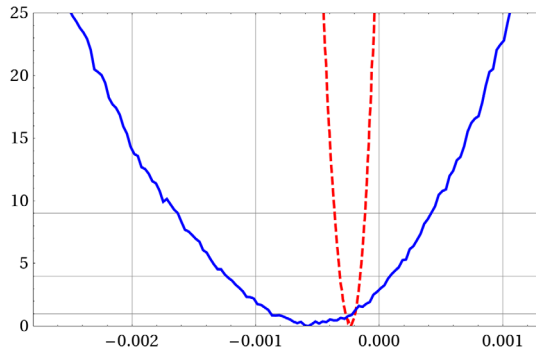


FIG. 3 (color online). $\Delta\chi^2$ profile of A_{SL}^b ; the blue line corresponds to the NP scenario; the red dashed line corresponds to the SM case. The last D0 measurements give $A_{\text{SL}}^b = (-4.96 \pm 1.69) \times 10^{-3}$ [1].

even if this enhancement softens the disagreement with the experimental value of A_{SL}^b , that central value is out of the ranges that this new physics scenario can accommodate. For completeness we display in Fig. 4 the $\Delta\chi^2$

profiles for the combinations $A_{\text{SL}}^s \pm A_{\text{SL}}^d$, of interest for the LHCb experiment. The potential enhancement with respect to SM expectations in Eq. (21) is, once again, noticeable:

$$\begin{aligned} A_{\text{SL}}^s + A_{\text{SL}}^d &= (-1.0 \pm 0.6) \times 10^{-3}, \\ A_{\text{SL}}^s - A_{\text{SL}}^d &= (1.0 \pm 0.7) \times 10^{-3}. \end{aligned}$$

It should be stressed that deviating from SM expectations in A_{SL}^d and in A_{SL}^s is intimately related to NP effects in other observables. For A_{SL}^d , large values are associated to “tensions” in bd that manifest, for example, through larger than standard values of $|V_{ub}|$. This is illustrated through the correlated $\Delta\chi^2$ profiles of A_{SL}^d vs $|V_{ub}|$ shown in Fig. 5(a). On the other hand, for A_{SL}^s , large values of A_{SL}^s are associated to large values of the CP asymmetry $A_{J/\Psi\Phi}$, as Fig. 5(b) confirms [and could be anticipated from Fig. 2(b)]. The dimuon asymmetry A_{SL}^b is sensitive to both correlations, as Figs. 5(c) and 5(d) illustrate.

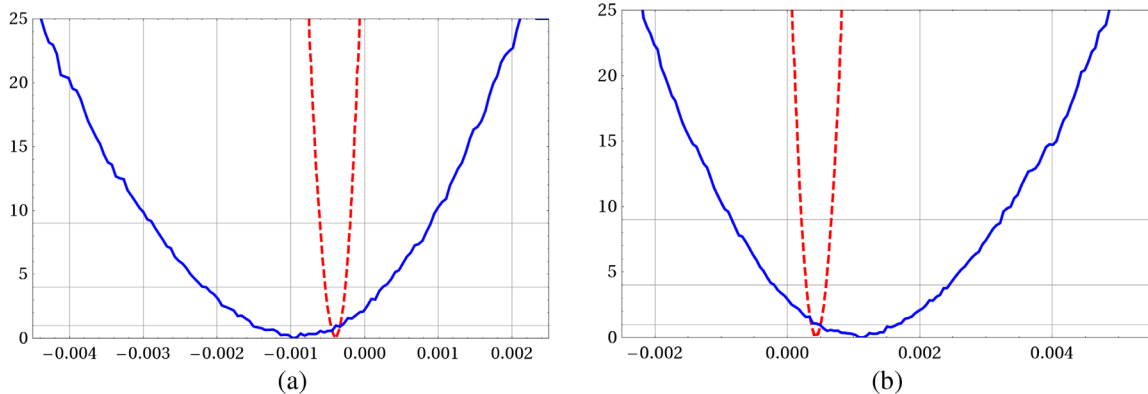


FIG. 4 (color online). $\Delta\chi^2$ profile of the combinations of semileptonic asymmetries $A_{\text{SL}}^s \pm A_{\text{SL}}^d$; the blue lines correspond to the NP scenario—Eq. (22)—the red dashed lines correspond to the SM case. (a) $\Delta\chi^2$ vs $A_{\text{SL}}^s + A_{\text{SL}}^d$. (b) $\Delta\chi^2$ vs $A_{\text{SL}}^s - A_{\text{SL}}^d$.

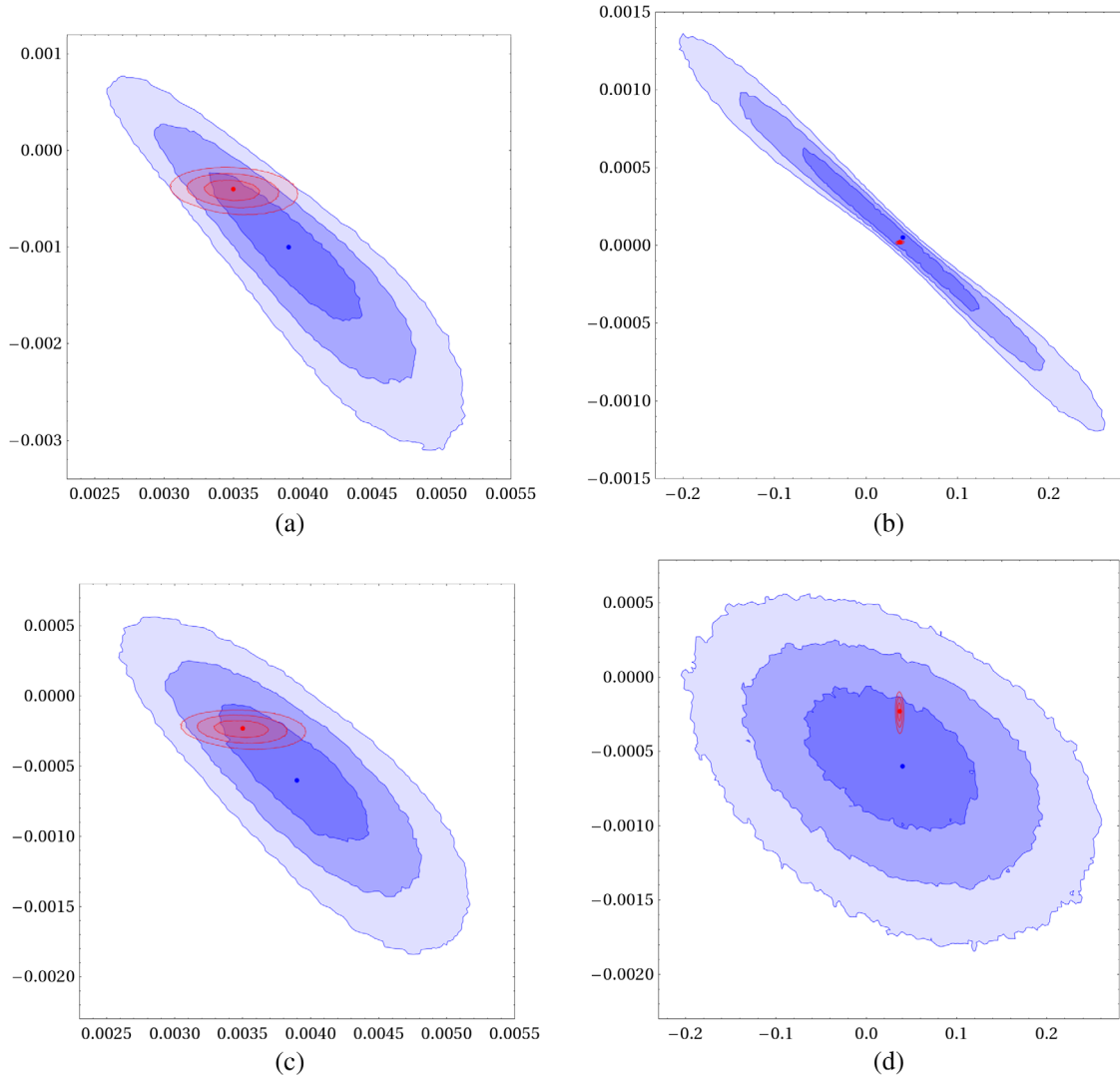


FIG. 5 (color online). $\Delta\chi^2$ 68%, 95% and 99% C.L. regions. Blue regions correspond to the NP scenario; red regions correspond to the SM case. Notice that with the scales in Fig. 5(b), the SM region is barely a point. (a) A_{SL}^d vs $|V_{ub}|$. (b) A_{SL}^s vs $A_{J/\psi K_S}$. (c) A_{SL}^b vs $|V_{ub}|$. (d) A_{SL}^b vs $A_{J/\psi\Phi}$.

Along this section we have analyzed in detail how the introduction of new physics in the mixings $M_{12}^{(q)}$ allows for significant deviations from SM expectations in the semi-leptonic asymmetries A_{SL}^q . The key point at the origin of those deviations is the effect of the phases ϕ_q : (1) within the SM, 3×3 unitarity and the top quark dominance of $M_{12}^{(q)}$ together, enforce a natural suppression of A_{SL}^d and A_{SL}^s ; (2) the presence of $\phi_q \neq 0$ misaligns the phases of the would-be leading contribution to $\Gamma_{12}^{(q)}$ (the one not suppressed by m_c/m_b) and $M_{12}^{(q)}$; (3a) in the $B_s^0-\bar{B}_s^0$ system, since $[A_{J/\psi\Phi}]_{SM} \sim \mathcal{O}(10^{-2})$, but the experimental sensitivity has just started to explore that ground, there is still ample room for $\phi_s \neq 0$, and thus $A_{SL}^s \sim \mathcal{O}(10^{-3})$ can be achieved; (3b) in the $B_d^0-\bar{B}_d^0$ system, $A_{J/\psi K_S} \approx 0.68$ has

been measured to a few-percent precision; in addition, unitarity imposes a close relation between $|V_{ub}|$ and β that is transmitted, within the SM, to $A_{J/\psi K_S}$. Having $\phi_d \neq 0$ requires, necessarily, that both $|V_{ub}|$ and β deviate from their SM values while $A_{J/\psi K_S}$ remains unchanged. The presence of “tensions” between the $|V_{ub}|$ and the $A_{J/\psi K_S}$ measurements favors, in this simple NP scenario, $\phi_d \neq 0$, thus evading the SM suppression and obtaining a significant enhancement of A_{SL}^d . New physics at the 20%–30% level in $M_{12}^{(d)}$ does not give a 20%–30% modification in A_{SL}^d ; it gives a much larger effect, contrary to what one can naively expect [12]. It should be stressed that, despite the significant increase with respect to the SM, the values that can be reached for A_{SL}^d and A_{SL}^s are too small to reproduce the D0 value of the A_{SL}^b asymmetry.

IV. NEW PHYSICS BEYOND 3×3 UNITARITY

The model-independent parametrizations in Eq. (22) do not exhaust the NP scenarios that could give rise to an enhancement of the mixing asymmetries A_{SL}^d and A_{SL}^s . One can consider scenarios in which the CKM matrix is no longer 3×3 unitary and it is, on the contrary, part of a larger unitary matrix. If the CKM matrix is part of a larger unitary matrix, there are, necessarily, additional fields beyond the standard three chiral ones; since they may couple to known quarks and weak bosons, they can give new contributions to $M_{12}^{(q)}$, controlled by the matrix elements beyond the 3×3 usual CKM matrix. If, for instance,

$$V_{ub}V_{uq}^* + V_{cb}V_{cq}^* + V_{tb}V_{tq}^* \equiv -N_{bq} \neq 0, \quad (31)$$

one should consider modified $M_{12}^{(q)}$ expressions with the following structure [30]:

$$M_{12}^{(q)} = \frac{G_F^2 M_W^2}{12\pi^2} M_{B_q} f_{B_q}^2 B_{B_q} \eta_B ((V_{ib}V_{iq}^*)^2 S_0(x_t) + (V_{tb}V_{tq}^*) N_{bq} C_1 + N_{bq}^2 C_2). \quad (32)$$

C_1 and C_2 , both real, are the model-dependent parameters that control the terms linear and quadratic (respectively) in the deviation N_{bq} of the mixing matrix with respect to 3×3 unitarity. We consider C_1 and C_2 common to both $M_{12}^{(d)}$ and $M_{12}^{(s)}$, and real, confining all the new flavor dependence and CP violation to the mixings N_{bq} . Examples of such scenarios are models where the fermion content is extended through additional chiral or vectorlike quarks [30,31]. Equations (31) and (32) provide indeed the ingredients analyzed in the previous section that could induce deviations from SM expectations both in A_{SL}^d and in A_{SL}^s [30,31]. Notice that we include new terms in $M_{12}^{(q)}$, not in $\Gamma_{12}^{(q)}$. To include new terms in $\Gamma_{12}^{(q)}$ one should expand the present analysis since those eventual new contributions would be model dependent and constrained by additional information concerning $\Delta B \neq 0$ processes, as done, e.g. in [14,32]. Since the simplest realization of this extended scenario is to consider the CKM matrix to be embedded in a 4×4 unitary matrix, we restrict our analyses of the next subsections to such a case. Then, Eq. (31) gives

$$\lambda_{bq}^u + \lambda_{bq}^c + \lambda_{bq}^t = -\lambda_{bq}^4, \quad q = d, s, \quad (33)$$

where U is 4×4 unitary, $U_{ij} = V_{ij}$ for $i, j \leq 3$ and $\lambda_{bq}^a \equiv V_{ab}V_{aq}^*$. The B_q^0 - \bar{B}_q^0 mixing amplitude $M_{12}^{(q)}$ is

$$M_{12}^{(q)} = \frac{G_F^2 M_W^2}{12\pi^2} m_{B_q} f_{B_q}^2 B_{B_q} \eta_B \times ((\lambda_{bq}^t)^2 S_0(x_t) + 2(\lambda_{bq}^t \lambda_{bq}^4) C_1 + (\lambda_{bq}^4)^2 C_2). \quad (34)$$

Then, instead of Eq. (9), we have

$$\frac{\Gamma_{12}^{(q)}}{M_{12}^{(q)}} = K_{(q)} S_0(x_t) \times \left[\frac{c(\lambda_{bq}^u + \lambda_{bq}^c)^2 - a\lambda_{bq}^u(\lambda_{bq}^u + \lambda_{bq}^c) + b(\lambda_{bq}^u)^2}{(\lambda_{bq}^t)^2 S_0(x_t) + 2(\lambda_{bq}^t \lambda_{bq}^4) C_1 + (\lambda_{bq}^4)^2 C_2} \right], \quad (35)$$

and unitarity—Eq. (33)—allows us to write the first term as

$$c \frac{(\lambda_{bq}^t + \lambda_{bq}^4)^2}{(\lambda_{bq}^t)^2 S_0(x_t) + 2(\lambda_{bq}^t \lambda_{bq}^4) C_1 + (\lambda_{bq}^4)^2 C_2}, \quad (36)$$

which is not, in general, real. In this kind of new physics scenario, the SM suppression of A_{SL}^q is naturally removed: the two ingredients which align the phase of this would-be-leading term with that of $M_{12}^{(q)}$, namely 3×3 unitarity and $M_{12}^{(q)}$ dominated by the top quark contribution, are absent. In order to illustrate how deviations of 3×3 unitarity provide the ingredients that may enhance the semileptonic asymmetries, Figs. 9 and 10 in Appendix B show the modifications brought by this scenario with respect to the previous 3×3 unitary one and with respect to the SM. The analysis of Sec. III is rather simple and general, because of the complete parametric freedom and independence accorded to r_d , r_s , ϕ_d and ϕ_s . The present scenario with a 4×4 unitary mixing is somehow different: besides C_1 and C_2 , all the available freedom is the freedom that 4×4 unitarity provides to have bd and bs quadrangles instead of triangles. For specific models, C_1 and C_2 will have well-defined functional forms (involving new fermion masses, for example): to maintain full generality, C_1 and C_2 are allowed to vary freely within reasonable ranges, in particular we consider [33] $C_1 \in [-10; 10]$ and $C_2 \in [-10^3; 10^3]$.

The previous prospects translate into results for the relevant observables: Fig. 6 shows the $\Delta\chi^2$ profiles of A_{SL}^d and A_{SL}^s , together with the ones corresponding to the NP scenario of Sec. III and the SM ones for easy comparison. The values that the semileptonic asymmetries may reach are similar to the ones that can be obtained in the 3×3 unitary scenario with NP in $M_{12}^{(q)}$. With the results for the single A_{SL}^d and A_{SL}^s asymmetries, one can expect the dimuon asymmetry A_{SL}^b to span a range similar to the one in Fig. 3: Fig. 6(c) shows the $\Delta\chi^2$ profile of A_{SL}^b for the 4×4 unitary case, together with the ones in Fig. 3 for

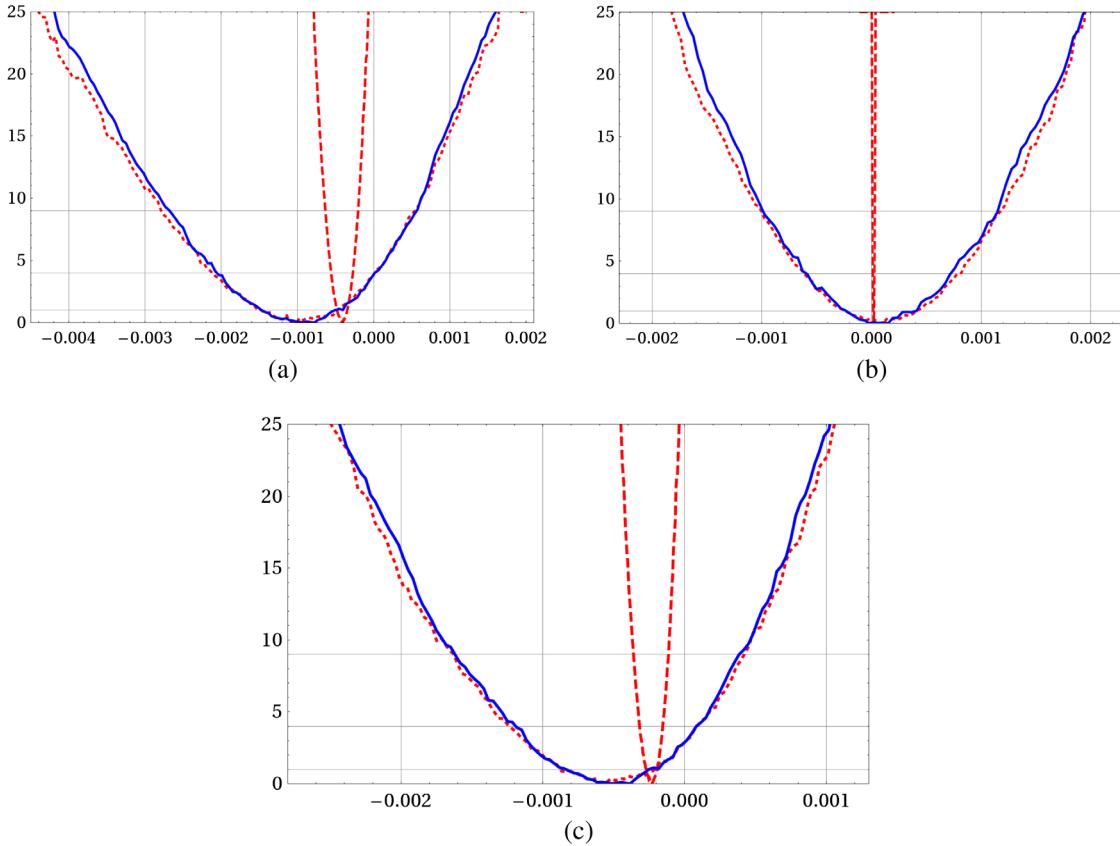


FIG. 6 (color online). $\Delta\chi^2$ profiles of semileptonic asymmetries A_{SL}^q ; the blue lines correspond to the 4×4 unitary NP scenario—Eqs. (33) and (34)—the red dotted lines correspond to the 3×3 unitary NP scenario of Sec. III; the red dashed lines correspond to the SM case. The last D0 measurement gives $A_{\text{SL}}^b = (-4.96 \pm 1.69) \times 10^{-3}$ [1]. (a) $\Delta\chi^2$ vs A_{SL}^d . (b) $\Delta\chi^2$ vs A_{SL}^s . (c) $\Delta\chi^2$ vs A_{SL}^b .

comparison. As in the 3×3 unitary case with NP in $M_{12}^{(q)}$, the value of A_{SL}^b is enhanced, thus reducing the discrepancy with the D0 result, but the enhancement is insufficient to reproduce the measurement.

This confirms the basic picture that underlies deviations from SM expectations and establishes deviations from 3×3 unitarity as a framework that accommodates them naturally: in the bd sector, A_{SL}^d values at the 10^{-3} level can be reached when the tight connection between $|V_{ub}|$ and $A_{J/\psi K_S}$ present in the SM is relaxed; in the bs sector, A_{SL}^s values at the 10^{-3} level can be reached when $A_{J/\psi\Phi}$ deviates from the SM expectation $A_{J/\psi\Phi} \approx 0.04$. Both ingredients are present in this NP scenario with the CKM matrix part of a larger 4×4 unitary matrix, as Figs. 7(a) and 7(b) illustrate. This behavior is inherited by A_{SL}^b : deviations in A_{SL}^b from SM expectations are correlated, as in the 3×3 unitary case with NP in $M_{12}^{(q)}$, with deviations in $|V_{ub}|$ and $A_{J/\psi\Phi}$, as Figs. 7(c) and 7(d) illustrate.

A. Deviations from 3×3 unitarity

In Secs. III and IV we have explored two NP avenues that induce deviations in A_{SL}^d and A_{SL}^s . The experimental constraints entering both analyses are (i) tree level

measurements of the mixing matrix (moduli $|V_{ij}|$ of the first two rows and the phase γ), and (ii) measurements of $B_d^0-\bar{B}_d^0$ and $B_s^0-\bar{B}_s^0$ mixings— ΔM_{B_d} , ΔM_{B_s} and the effective phases $2\bar{\beta}$ (through $A_{J/\psi K_S}$) and $2\bar{\beta}_s$ (through $A_{J/\psi\Phi}$). An important question one can ask is the following: with those ingredients, to what extent could we distinguish the two NP scenarios? That is, could we uncover eventual deviations from 3×3 unitarity if they are indeed originating some discrepancy with respect to SM expectations?

In Figs. 9(a), 9(c) and 9(e), the tree level measurements “fix” the $|V_{ud}V_{ub}^*|$ and $|V_{cd}V_{cb}^*|$ sides, together with their relative orientation given by γ . Then ΔM_{B_d} and $A_{J/\psi K_S}$ “fix” the mixing in Figs. 9(b), 9(d) and 9(f). If there is some NP hint it will manifest through an incompatibility among related quantities, for example among the value of $|V_{td}V_{tb}^*|$ (controlling ΔM_{B_d}) and γ , or among the value of $|V_{cd}V_{cb}^*|$ and $\alpha = \pi - \gamma - \beta$, or among the value of $|V_{ud}V_{ub}^*|$ and β (this incompatibility is none other than the “ bd tension”). While this may seem straightforward, as soon as one concedes that only SM tree level dominated quantities are “safe” (not polluted by eventual NP contributions), none of these are useful: for the first, ΔM_{B_d} arises at one loop in the SM, invalidating the indirect obtention of $|V_{td}V_{tb}^*|$ from it [34]; for the second and third, the phases

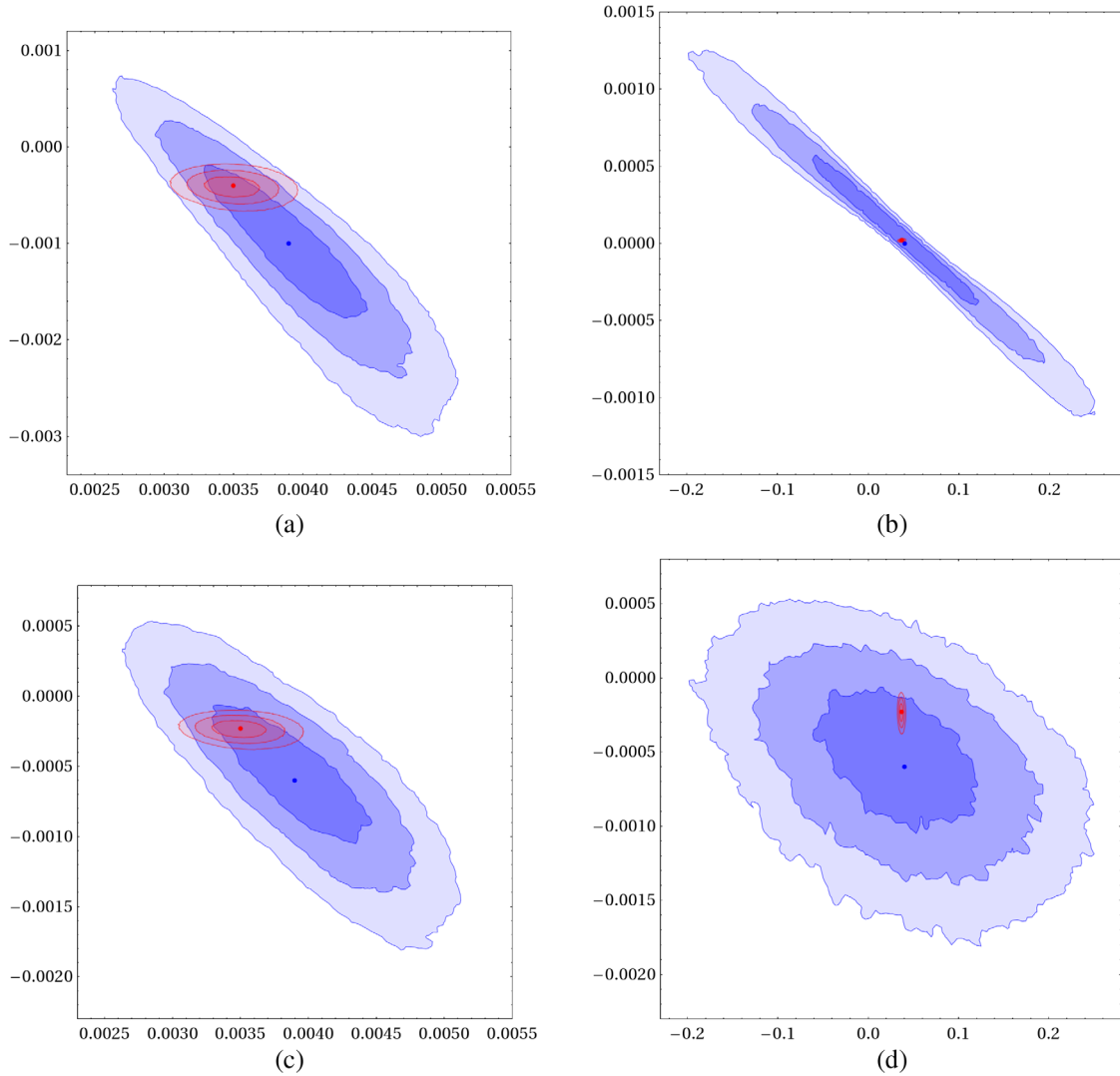


FIG. 7 (color online). $\Delta\chi^2$ 68%, 95% and 99% C.L. regions. Blue regions correspond to the 4×4 unitary NP scenario; red regions correspond to the SM case. (a) A_{SL}^d vs $|V_{ub}|$. (b) A_{SL}^s vs $A_{J/\Psi\Phi}$. (c) A_{SL}^b vs $|V_{ub}|$. (d) A_{SL}^b vs $A_{J/\Psi\Phi}$.

that are in fact measured are not β and α but the effective $\bar{\beta}$ and $\bar{\alpha} = \pi - \gamma - \bar{\beta}$, which may deviate from β , α through new contributions to $M_{12}^{(d)}$.

One can establish a tension with respect to the SM expectations, but this mismatch involves both the structure of the mixing matrix (the unitarity triangle) and the $M_{12}^{(d)}$ prediction: as soon as NP introduces new parameters that break the SM connection between both, the minimal set of observables that we are considering cannot indicate whether we have deviations from 3×3 unitarity or not [35]. The previous discussion concerns the bd sector, but the situation in the bs sector is not conceptually different. This does not mean that unitarity deviations cannot be established, it only means that the rather restricted set of observables that we are considering for this general analysis is not sufficient for that task, and the following roads have to be explored.

- (1) As soon as a specific model that incorporates mixings beyond the 3×3 unitary case is considered, a specific pattern of deviations with respect to SM expectations in flavor changing processes like $B_d \rightarrow X_s \gamma$, $B_d \rightarrow X_s \ell^+ \ell^-$, $B_{d,s} \rightarrow \mu^+ \mu^-$ —and others outside B mesons systems like $K_L \rightarrow \mu^+ \mu^-$, $K \rightarrow \pi \nu \bar{\nu}$ or $K^0 - \bar{K}^0$ and $D^0 - \bar{D}^0$ oscillations—will emerge, and a much larger set of experimental measurements can be used.
- (2) On the other hand, deviations from 3×3 unitarity may be directly probed through
 - (a) $|V_{tb}| \neq 1$ at the percent level, which would be within the sensitivity of the LHC experiments [36–38],
 - (b) $|V_{ud}|^2 + |V_{us}|^2 + |V_{ub}|^2 \neq 1$, and
 - (c) $|V_{cd}|^2 + |V_{cs}|^2 + |V_{cb}|^2 \neq 1$.

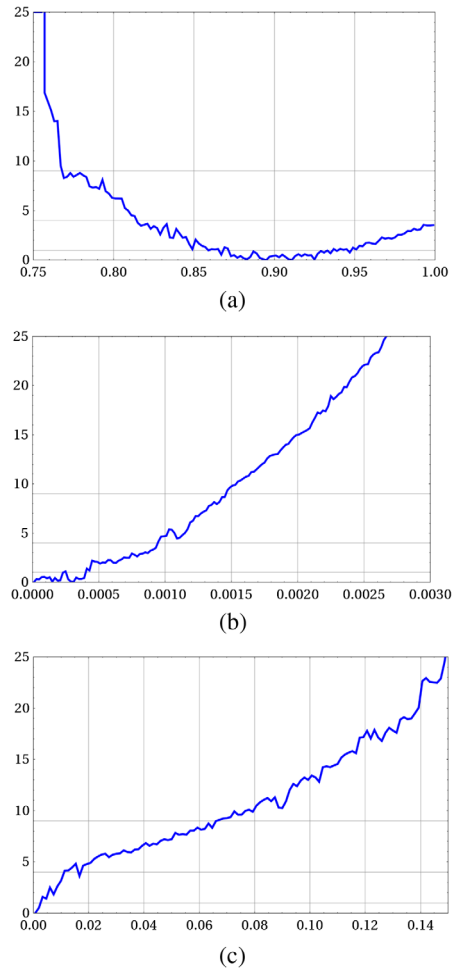


FIG. 8 (color online). $\Delta\chi^2$ profiles of the deviations from 3×3 unitarity in $|V_{tb}|$ and in the first and second rows of the mixing matrix. (a) $\Delta\chi^2$ vs $|V_{tb}|$. (b) $\Delta\chi^2$ vs $1 - |V_{ud}|^2 - |V_{us}|^2 - |V_{ub}|^2$. (c) $\Delta\chi^2$ vs $1 - |V_{cd}|^2 - |V_{cs}|^2 - |V_{cb}|^2$.

The first possibility followed for example in [12] is completely model specific and thus of no use for the present model-independent approach. For the second possibility, we can directly explore to which extent all three signals of deviation from 3×3 unitarity may arise. This is illustrated in Fig. 8. In Fig. 8(a) one can actually observe that $|V_{tb}|$ can depart from the $1 - \mathcal{O}(10^{-4})$ ballpark that 3×3 unitarity imposes, and do so at a level which the LHC experiments can probe. In Figs. 8(b) and 8(c) the deviation from 3×3 unitarity in the first (u) and second (c) rows of the mixing matrix are displayed: in both cases deviations from 3×3 unitarity at a level to be explored in the near future are allowed within our framework.

V. CONCLUSIONS

Within the SM, the CP -violating asymmetries A_{SL}^d and A_{SL}^s in the neutral $B_d^0-\bar{B}_d^0$ and $B_s^0-\bar{B}_s^0$ mixings are expected to be naturally small.

The D0 Collaboration has measured the like-sign dimuon asymmetry A_{SL}^b —which is a combination of the A_{SL}^d and A_{SL}^s asymmetries—and obtained a large value, marginally compatible (at around the 3σ level) with the SM expectations. Since this fact might hint to new physics, we have considered two different NP scenarios. In the well-known first scenario the CKM mixing matrix remains 3×3 unitary and NP enters $B_d^0-\bar{B}_d^0$ and $B_s^0-\bar{B}_s^0$ mixings in a simple parametric manner. In the second scenario, which we analyzed for the first time in detail, deviations from 3×3 unitarity in the mixing matrix are allowed, and they are related to new contributions to B meson mixings. In both scenarios A_{SL}^d and A_{SL}^s can be sizably enhanced with respect to SM expectations. In the case of A_{SL}^d , nonstandard values are related to the tension between $|V_{ub}|$ and $A_{J/\psi K_S}$: NP alleviates that tension and, modifying $M_{12}^{(d)}$ at the 20%–30% level, can increase A_{SL}^d fivefold. The case where A_{SL}^s is different: as NP crucially changes the relation between the phase β_s and $A_{J/\psi\Phi}$, A_{SL}^s is allowed to reach values almost 2 orders of magnitude larger than the SM expectation. In A_{SL}^s too, deviations from SM expectations are related to other NP effects: $A_{J/\psi\Phi}$ in this case. When both A_{SL}^d and A_{SL}^s are enhanced, A_{SL}^b may reach values at the 10^{-3} to 2×10^{-3} level. Nevertheless, obtaining a prediction 5 times larger than in the SM is not enough to reproduce the D0 measurement of A_{SL}^b . Meanwhile, experimental results from the LHCb experiment are eagerly awaited to put some light on the issue. The SM predictions for A_{SL}^d and A_{SL}^s are really tight: a measurement that sees an increase in one or both will point, undoubtedly, to NP and new sources of CP violation.

ACKNOWLEDGMENTS

This work was supported by Spanish MINECO under Grant No. FPA2011-23596, by Generalitat Valenciana under Grant No. GVPROMETEOII 2014-049 and by Fundação para a Ciência e a Tecnologia (FCT, Portugal) through the Projects No. CERN/FP/83503/2008, No. EXPL/FIS-NUC/0460/2013 and No. CFTP-FCT Unit 777 (PEst-OE/FIS/UI0777/2011) which are partially funded through POCTI (FEDER).

APPENDIX A: INPUT

Table I summarizes the experimental input [1,4,39–49] used for the different calculations; measurements are interpreted as Gaussians with the quoted values for the central value and the uncertainty. The $\Delta\chi^2$ profiles and regions have been computed through adapted Markov Chain Monte Carlo techniques that allow for an efficient exploration of the different parameter spaces. For the additional theoretical input from lattice QCD, $f_{B_s}\sqrt{B_{B_s}} = 266 \pm 18$ MeV and $\xi \equiv \frac{f_{B_s}\sqrt{B_{B_s}}}{f_{B_d}\sqrt{B_{B_d}}} = 1.268 \pm 0.063$ have

TABLE I. Experimental input [N.B. $R_t \equiv |V_{tb}|^2 / (|V_{td}|^2 + |V_{ts}|^2 + |V_{tb}|^2)$].

$ V_{ud} $	0.97425 ± 0.00022	$ V_{us} $	0.2252 ± 0.0009	$ V_{ub} $	0.00375 ± 0.00040
$ V_{cd} $	0.230 ± 0.011	$ V_{cs} $	1.023 ± 0.036	$ V_{cb} $	0.041 ± 0.001
R_t	0.90 ± 0.05				
γ	$(68 \pm 8)^\circ$	$A_{J/\Psi K_S}$	0.68 ± 0.02	$A_{J/\Psi \Phi}$	0.01 ± 0.07
$\sin(2\bar{\alpha})$	0.00 ± 0.14	$\sin(2\bar{\beta} + \gamma)$	0.95 ± 0.40		
ΔM_{B_d}	$(0.507 \pm 0.004) \text{ ps}^{-1}$	$\Delta \Gamma_d$	$(-0.011 \pm 0.014) \text{ ps}^{-1}$	A_{SL}^d	$(3 \pm 23) \times 10^{-4}$
ΔM_{B_s}	$(17.768 \pm 0.024) \text{ ps}^{-1}$	$\Delta \Gamma_s$	$(0.091 \pm 0.008) \text{ ps}^{-1}$	A_{SL}^s	$(-32 \pm 52) \times 10^{-4}$
A_{SL}^b [1]	$(-4.96 \pm 1.69) \times 10^{-3}$				

been used [50]; although the results presented correspond to modeling the theoretical uncertainties in a Gaussian manner, it has been checked that modeling them with uniform uncertainties restricted to 1σ or 2σ ranges produces no change.

APPENDIX B: UNITARITY AND MIXINGS

Figures 9(a) and 9(b) show the unitarity triangle bd (in the complex plane) and $\Delta M_{B_d} e^{i2\bar{\beta}}$ (that is $M_{12}^{(d)}$) for the SM

case. The “ bd tension” is, schematically, the coincidence of an experimental value of $|V_{ub}|$ which pushes towards larger values than the represented (illustrative) case, with an experimental value of $A_{J/\Psi K_S} = \sin(2\bar{\beta})$ which pulls in the opposite direction. In Figs. 9(c) and 9(d), we illustrate the analysis of Sec. III: the presence of NP alleviates the tension allowing for larger $|V_{ub}|$ values, which trigger the sizable deviations in A_{SL}^d , from SM expectations, which we are interested in. Figures 9(e) and 9(f) illustrate the non- (3×3) unitary scenario. In particular, Fig. 9(e) displays the

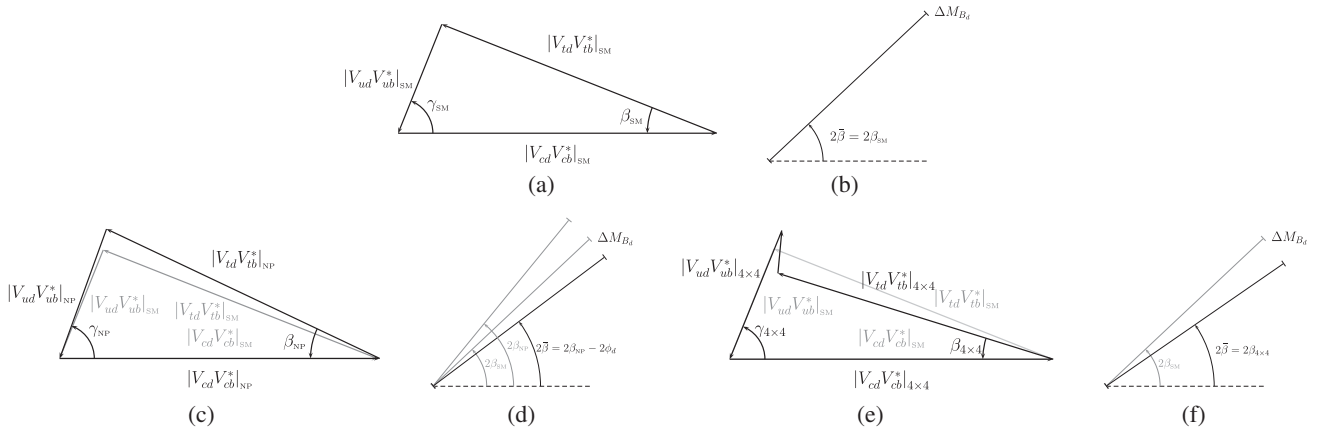


FIG. 9. bd unitarity and $M_{12}^{(d)}$ in the SM and beyond. (a) bd unitarity triangle in the SM. (b) $M_{12}^{(d)}$ in the SM. (c) bd unitarity triangle with NP in mixings. (d) $M_{12}^{(d)}$ with NP. (e) bd unitarity quadrangle. (f) $M_{12}^{(d)}$ beyond 3×3 unitarity.

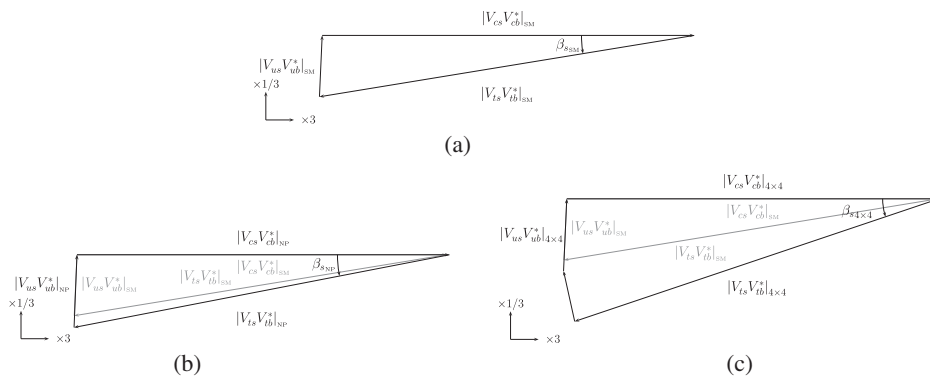


FIG. 10. bs unitarity and $M_{12}^{(s)}$ in the SM and beyond. (a) bs unitarity triangle in the SM. (b) bs unitarity triangle with NP in mixings. (c) bs unitarity quadrangle.

unitarity quadrangle bd corresponding to the enlarged 4×4 unitary mixing matrix. One can easily see how the presence of the fourth side, i.e. deviation from 3×3 unitarity, permits larger $|V_{ub}|$ values. Figure 9(f) shows how the corresponding mixing gives adequate values for ΔM_{B_d} and $A_{J/\Psi K_S}$. For the bs case, Fig. 10 illustrates the situation (we omit $M_{12}^{(s)}$ for conciseness): Fig. 10 is just the SM squashed unitarity triangle bs ; it does not change much

(as analyzed in Sec. III) upon inclusion of NP in $M_{12}^{(q)}$, as Fig. 10(b) shows: the relevant contribution in that case is directly provided by NP through ϕ_s . Finally, Fig. 10(c) shows how the departure from 3×3 unitarity may induce significant departures in the value of the phase β_s entering $M_{12}^{(s)}$, as required to depart from SM values of A_{SL}^s (and $A_{J/\Psi\Phi}$).

-
- [1] V.M. Abazov *et al.* (D0 Collaboration), *Phys. Rev. D* **84**, 052007 (2011); **89**, 012002 (2014).
- [2] We directly refer in the following to *muons* since they are the cleanest case from the experimental point of view.
- [3] Although central in any experimental analysis, we omit any discussion on issues such as efficiencies or backgrounds.
- [4] J. Lees *et al.* (BABAR Collaboration), *Phys. Rev. Lett.* **111**, 101802 (2013); Addendum **111**, 159901 (2013); R. Aaij *et al.* (LHCb Collaboration), *Phys. Lett. B* **728**, 607 (2014).
- [5] Nevertheless, as we will show, since significant cancellations are at work in the SM case, large NP contributions are not necessary to obtain significant enhancements in A_{SL}^d .
- [6] P. Ko and J.-h. Park, *Phys. Rev. D* **82**, 117701 (2010); J. Parry, *Phys. Lett. B* **694**, 363 (2011); H. Ishimori, Y. Kajiyama, Y. Shimizu, and M. Tanimoto, *Prog. Theor. Phys.* **126**, 703 (2011).
- [7] A. Datta, M. Duraisamy, and S. Khalil, *Phys. Rev. D* **83**, 094501 (2011); F. Goertz and T. Pfoh, *Phys. Rev. D* **84**, 095016 (2011).
- [8] N. Deshpande, X.-G. He, and G. Valencia, *Phys. Rev. D* **82**, 056013 (2010); A. K. Alok, S. Baek, and D. London, *J. High Energy Phys.* 07 (2011) 111; J. E. Kim, M.-S. Seo, and S. Shin, *Phys. Rev. D* **83**, 036003 (2011); H. D. Kim, S.-G. Kim, and S. Shin, *Phys. Rev. D* **88**, 015005 (2013).
- [9] K. Y. Lee and S.-h. Nam, *Phys. Rev. D* **85**, 035001 (2012).
- [10] M. Jung, A. Pich, and P. Tuzon, *J. High Energy Phys.* 11 (2010) 003; B. A. Dobrescu, P. J. Fox, and A. Martin, *Phys. Rev. Lett.* **105**, 041801 (2010); M. Trott and M. B. Wise, *J. High Energy Phys.* 11 (2010) 157; Y. Bai and A. E. Nelson, *Phys. Rev. D* **82**, 114027 (2010).
- [11] C.-H. Chen and G. Faisel, *Phys. Lett. B* **696**, 487 (2011).
- [12] W.-S. Hou and N. Mahajan, *Phys. Rev. D* **75**, 077501 (2007); A. Soni, A. K. Alok, A. Giri, R. Mohanta, and S. Nandi, *Phys. Rev. D* **82**, 033009 (2010); C.-H. Chen, C.-Q. Geng, and W. Wang, *J. High Energy Phys.* 11 (2010) 089; F. J. Botella, G. C. Branco, and M. Nebot, *Phys. Rev. D* **79**, 096009 (2009); F. Botella, G. Branco, and M. Nebot, *J. High Energy Phys.* 12 (2012) 040; A. K. Alok and S. Gangal, *Phys. Rev. D* **86**, 114009 (2012); A. K. Alok, S. Banerjee, D. Kumar, and S. U. Sankar, arXiv:1402.1023.
- [13] Z. Ligeti, M. Papucci, G. Perez, and J. Zupan, *Phys. Rev. Lett.* **105**, 131601 (2010); C. W. Bauer and N. D. Dunn, *Phys. Lett. B* **696**, 362 (2011).
- [14] C. Bobeth and U. Haisch, *Acta Phys. Pol. B* **44**, 127 (2013); C. Bobeth, U. Haisch, A. Lenz, B. Pecjak, and G. Tetlalmatzi-Xolocotzi, *J. High Energy Phys.* 06 (2014) 040.
- [15] S. Descotes-Genon and J. F. Kamenik, *Phys. Rev. D* **87**, 074036 (2013).
- [16] G. C. Branco, L. Lavoura, and J. P. Silva, *CP Violation* (Oxford University Press, Oxford, 1999), Vol. 103, pp. 1–536.
- [17] Equation (4) includes perturbative QCD corrections η_B , and nonperturbative information, i.e. the decay constant f_{B_q} and the bag parameter B_q . Subleading contributions from virtual u or c quarks are neglected.
- [18] M. Beneke, G. Buchalla, C. Greub, A. Lenz, and U. Nierste, *Phys. Lett. B* **459**, 631 (1999); M. Beneke, G. Buchalla, A. Lenz, and U. Nierste, *Phys. Lett. B* **576**, 173 (2003); M. Ciuchini, E. Franco, V. Lubicz, F. Mescia, and C. Tarantino, *J. High Energy Phys.* 08 (2003) 031; A. Lenz, arXiv:1205.1444; J. Hagelin, *Nucl. Phys.* **B193**, 123 (1981).
- [19] A. Lenz and U. Nierste, *J. High Energy Phys.* 06 (2007) 072.
- [20] F. J. Botella, G. C. Branco, and M. Nebot, *Nucl. Phys.* **B768**, 1 (2007).
- [21] In both $B_d^0-\bar{B}_d^0$ and $B_s^0-\bar{B}_s^0$ systems, $\Delta M_{B_q} = 2|M_{12}^{(q)}|$ since $|\Gamma_{12}^{(q)}| \ll |M_{12}^{(q)}|$ [16].
- [22] Notice that Eq. (15) is written, as it should, in terms of quantities invariant under rephasings of the CKM elements and of the B_d^0 and \bar{B}_d^0 states, even if, for the sake of brevity, intermediate expressions such as Eq. (14) are not.
- [23] Besides $2\bar{\beta}$ from the golden channel $B_d \rightarrow J/\Psi K_S$, γ is accessed through *tree* level decays such as $B_d \rightarrow DK$, while the combination $2(\bar{\beta} + \gamma)$ is obtained in decay channels $B_d \rightarrow \pi\pi, \rho\pi, \rho\rho$.
- [24] T. Bird (LHCb collaboration), *J. Phys. Conf. Ser.* **447**, 012021 (2013).
- [25] S. Laplace, Z. Ligeti, Y. Nir, and G. Perez, *Phys. Rev. D* **65**, 094040 (2002); Z. Ligeti, M. Papucci, and G. Perez, *Phys. Rev. Lett.* **97**, 101801 (2006); P. Ball and R. Fleischer, *Eur. Phys. J. C* **48**, 413 (2006); Y. Grossman, Y. Nir, and G. Raz, *Phys. Rev. Lett.* **97**, 151801 (2006); M. Bona *et al.* (UTfit Collaboration), *Phys. Rev. Lett.* **97**, 151803 (2006); F. Botella, G. Branco, M. Nebot, and M. Rebelo, *Nucl. Phys.* **B725**, 155 (2005); M. Bona *et al.* (UTfit Collaboration), *J. High Energy Phys.* 03 (2008) 049; A. Lenz, U. Nierste, J. Charles, S. Descotes-Genon, H. Lacker, S. Monteil, V. Niess, and S. T'Jampens, *Phys. Rev. D* **86**, 033008 (2012).

- [26] Another popular alternative uses the NP parameters h_q and σ_q with $r_q^2 e^{-i2\phi_q} \equiv 1 + h_q e^{i2\sigma_q}$, where this separation of NP is less straightforward. Our results, in any case, do not depend on adopting one parametrization or the other.
- [27] In fact, *tightly* constrained, except for the argument of $M_{12}^{(s)}$, accessed through $B_s \rightarrow J/\Psi\Phi$, where, despite the excellent performance of LHCb, the smallness of the SM expectation still allows for deviations.
- [28] M. Bona *et al.* (UTfit Collaboration), *Phys. Lett. B* **687**, 61 (2010); E. Lunghi and A. Soni, *Phys. Lett. B* **697**, 323 (2011).
- [29] For these and successive two-dimensional $\Delta\chi^2$ profiles, we display, for clarity, 68%, 95% and 99% C.L. regions.
- [30] G. Barenboim and F. Botella, *Phys. Lett. B* **433**, 385 (1998); G. Barenboim, F. Botella, G. Branco, and O. Vives, *Phys. Lett. B* **422**, 277 (1998); G. Barenboim, F. Botella, and O. Vives, *Phys. Rev. D* **64**, 015007 (2001); *Nucl. Phys.* **B613**, 285 (2001); G. Eyal and Y. Nir, *J. High Energy Phys.* **09** (1999) 013.
- [31] P. H. Frampton, P. Hung, and M. Sher, *Phys. Rep.* **330**, 263 (2000).
- [32] G. Branco, P. Parada, T. Morozumi, and M. Rebelo, *Phys. Lett. B* **306**, 398 (1993).
- [33] Those are sufficiently generous ranges: for example, for an additional up quark T , we will have $C_1 \rightarrow S_0(x_t, x_T)$ and $C_2 \rightarrow S_0(x_T)$, ($x_T = m_T^2/M_W^2$), with a mass m_T ranging up to 5 TeV, $C_1 \leq 9.3$ and $C_2 \leq 980$.
- [34] For completeness, there are no direct measurements of $|V_{td}|$, and not very constraining ones of $|V_{tb}|$ (see Table I).
- [35] J. P. Silva and L. Wolfenstein, *Phys. Rev. D* **55**, 5331 (1997).
- [36] G. Aad *et al.* (ATLAS Collaboration), *Phys. Lett. B* **716**, 142 (2012).
- [37] S. Chatrchyan *et al.* (CMS Collaboration), *Phys. Rev. Lett.* **110**, 022003 (2013).
- [38] J. Adelman, B. Alvarez Gonzalez, Y. Bai, M. Baumgart, R. K. Ellis *et al.*, [arXiv:1309.1947](https://arxiv.org/abs/1309.1947).
- [39] V. M. Abazov *et al.* (D0 Collaboration), *Phys. Rev. D* **86**, 072009 (2012).
- [40] J. Beringer *et al.* (Particle Data Group), *Phys. Rev. D* **86**, 010001 (2012).
- [41] Y. Amhis *et al.* (Heavy Flavor Averaging Group), [arXiv:1207.1158](https://arxiv.org/abs/1207.1158).
- [42] R. Aaij *et al.* (LHCb Collaboration), *Phys. Lett. B* **707**, 497 (2012).
- [43] R. Aaij *et al.* (LHCb Collaboration), *Phys. Rev. Lett.* **108**, 101803 (2012).
- [44] R. Aaij *et al.* (LHCb Collaboration), *Phys. Rev. D* **87**, 112010 (2013).
- [45] R. Aaij *et al.* (LHCb Collaboration), *New J. Phys.* **15**, 053021 (2013).
- [46] I. Adachi *et al.* (Belle Collaboration), *Phys. Rev. Lett.* **110**, 131801 (2013).
- [47] J. Lees *et al.* (BABAR Collaboration), *Phys. Rev. D* **88**, 031102 (2013).
- [48] E. Nakano *et al.* (Belle Collaboration), *Phys. Rev. D* **73**, 112002 (2006).
- [49] B. Aubert *et al.* (BABAR Collaboration), *Phys. Rev. Lett.* **96**, 251802 (2006).
- [50] S. Aoki, Y. Aoki, C. Bernard, T. Blum, G. Colangelo *et al.*, *Eur. Phys. J. C* **74**, 2890 (2014).